Structure of a Histidine Ligand in the Photosynthetic Oxygen-Evolving Complex As Studied by Light-Induced Fourier Transform Infrared Difference Spectroscopy†

Takumi Noguchi,*,‡ Yorinao Inoue,‡ and Xiao-Song Tang§

Photosynthesis Research Laboratory, The Institute of Physical and Chemical Research (RIKEN), Wako, Saitama 351-0198, Japan, and Life Sciences Enterprise, E. I. du Pont de Nemours & Company, Wilmington, Delaware 19880-0173

Received March 18, 1999; Revised Manuscript Received June 1, 1999

ABSTRACT: Fourier transform infrared (FTIR) signals of a histidine side chain were identified in flash-induced S_2/S_1 difference spectra of the oxygen-evolving complex (OEC) of photosystem II (PS II) using PS II membranes from globally ^{15}N-labeled spinach and PS II core complexes from *Synechocystis* cells in which both the imidazole nitrogens of histidine were selectively labeled with ^{15}N. A negative band at 1113−1114 cm^{-1} was downshifted by 7 cm^{-1} upon both global ^{15}N-labeling and selective [^{15}N]His labeling, and assigned to the C−N stretching mode of the imidazole ring. This band was unaffected by H−D exchange in the PS II preparations. In addition, several peaks observed at 2500−2850 cm^{-1} all downshifted upon global and selective ^{15}N-labeling. These were ascribed to Fermi resonance peaks on a hydrogen-bonding N−H stretching band of the histidine side chain. FTIR measurements of model compounds of the histidine side chain showed that the C−N stretching band around 1100 cm^{-1} can be a useful IR marker of the protonation form of the imidazole ring. The band appeared with frequencies in the following order: Nπ-protonated (>1100 cm^{-1}) > imidazolate > imidazolium > Nτ-protonated (<1095 cm^{-1}). The frequency shift upon N-deuteration was occurred in the following order: imidazolium (15−20 cm^{-1}) > Nτ-protonated (5−10 cm^{-1}) > Nπ-protonated ≈ imidazolate (∼0 cm^{-1}). On the basis of these findings together with the Fermi resonance peaks at >2500 cm^{-1} as a marker of N−H hydrogen-bonding, we concluded that the histidine residue in the S_2/S_1 spectrum is protonated at the Nπ site and that this Nπ-H is hydrogen bonded. This histidine side chain probably ligated the redox-active Mn ion at the Nτ site, and thus, oxidation of the Mn cluster upon S_2 formation perturbed the histidine vibrations, causing this histidine to appear in the S_2/S_1 difference spectrum.

Photosynthetic oxygen evolves on the electron-donor side of photosystem II (PS II).[1] The catalytic site is the oxygen-evolving complex (OEC) consisting of a tetranuclear Mn cluster, where two water molecules are oxidized to form one oxygen molecule and four protons. This reaction proceeds through a light-driven cycle of five intermediates, S_0-S_4, in which the S_1 state is dark stable and oxygen is evolved in the S_4-to-S_0 transition (*1*−*4*). The chemical mechanism of oxygen evolution, however, is not yet completely understood. The structure of the Mn cluster has been studied by EXAFS and EPR, and a dimer of a di-μ-oxo dimer has been proposed as the skeletal structure (*5*, *6*). Site-directed mutant (*7*−*11*) and chemical modification (*12*−*15*) studies suggested that aspartate, glutamate, and histidine side chains are involved in the amino acid ligands. Coordination of histidine residues has been also suggested by ESEEM and ENDOR studies (*16*, *17*), and ESEEM measurements using the cyanobacterium *Synechocystis* selectively labeled with ^{15}N at the nitrogen sites of the imidazole side chain of histidine residues (*18*) have provided further evidence of such coordination.

Light-induced FTIR difference spectroscopy is also a powerful means of investigating OEC structure and reactions. It directly detects the infrared absorption of individual amino acid residues as well as polypeptide chains, and thus can monitor their structural changes during photoreactions at the molecular level. FTIR spectroscopy is especially useful in detecting the hydrogen bonding interactions between polar groups that play important roles in enzymatic reactions, especially those involving proton transfer. FTIR spectra of OEC have been obtained as the difference between S_1 and S_2 states (*19*−*23*). Analyses of S_2/S_1 difference spectra have revealed carboxylate ligands (*19*−*22*), changes in conformations of the polypeptide chains (*19*, *21*, *22*), and structural coupling of a tyrosine residue with the Mn cluster (*23*).

† This research was supported by grants for Photosynthetic Sciences and Biodesign Research Program at The Institute of Physical and Chemical Research (RIKEN) provided by the Science and Technology Agency (STA) of Japan and was partially supported by the Central R&D Department of E. I. du Pont de Nemours & Co. (Contribution 7810).

* To whom correspondence should be addressed.

‡ The Institute of Physical and Chemical Research.

§ E. I. du Pont de Nemours & Co.

[1] Abbreviations: Cyt, cytochrome; ENDOR, electron nuclear double resonance; EPR, electron paramagnetic resonance; ESEEM, electron spin-echo envelope modulation; EXAFS, extended X-ray absorption fine structure; FePP(4-MeIm)$_2$, bis(4-methylimidazole) complex of iron protoporphyrin IX; FTIR, Fourier transform infrared; 4- and 5-MeIm, 4- and 5-methylimidazole, respectively; Mes, 2-(*N*-morpholino)ethanesulfonic acid; IR, infrared; OEC, oxygen-evolving complex; PS II, photosystem II; Q_A, primary quinone electron acceptor of PS II; Q_B, secondary quinone electron acceptor of PS II; Y_Z, redox-active tyrosine 161 of the D1 polypeptide.

10.1021/bi990631+ CCC: $18.00
Published on Web 07/08/1999

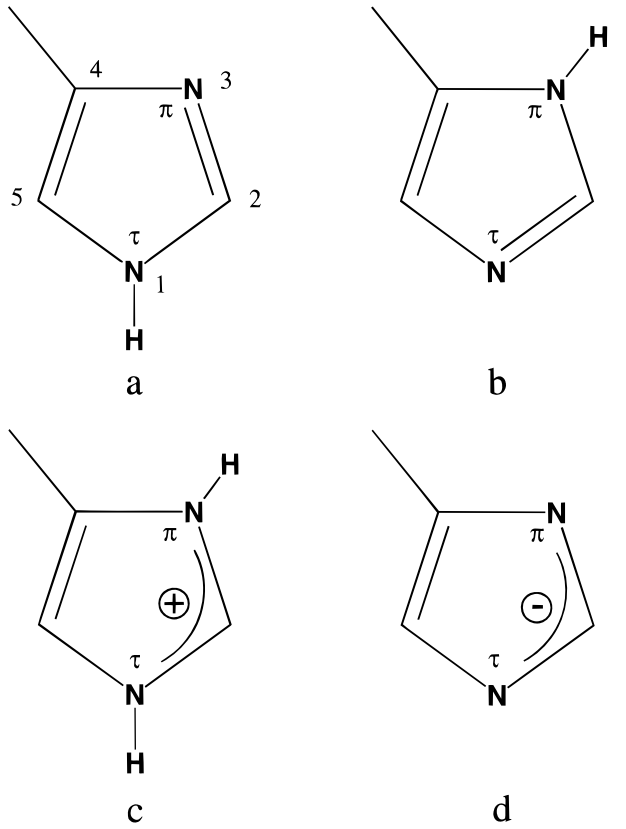

FIGURE 1: Structural diagram of a histidine side chain and 4- and 5-MeIm as model compounds: (a) Nτ-protonated form or 4-MeIm, (b) Nπ-protonated form or 5-MeIm, (c) imidazolium form, and (d) imidazolate form. In this study, numbering of atoms in all four forms of imidazole ring follows that of 4-MeIm. Note that according to the original numbering of 5-MeIm, the protonated nitrogen (Nπ) is numbered 1 and thus the methyl group is attached to C5.

The imidazole ring of a histidine side chain has two nitrogen atoms (Nτ and Nπ; see Figure 1) that serve as sites of protonation as well as of coordination to a metal ion(s). Thus, histidine is expected to be directly involved in the O_2-evolving reaction not only as a ligand of the Mn cluster but also as a mediator of proton transfer. It is therefore important to study the structures and reactions of histidine residues in the OEC to clarify the mechanism of O_2 evolution. To do so, the method of monitoring the histidine structure in the OEC during O_2 evolution must be established.

In this study, we identified histidine signals in the S_2/S_1 FTIR difference spectrum by global ^{15}N-labeling of PS II membranes from spinach and by selective ^{15}N-labeling of histidine side chains of PS II core particles from *Synechocystis* PCC 6803. In addition, measurements of model compounds of histidine side chains provided IR markers of protonation forms and hydrogen bonding interaction of the imidazole ring. The structure and interaction of the histidine residue in the OEC are discussed with reference to these markers.

MATERIALS AND METHODS

BBY-type O_2-evolving PS II membranes from spinach (*24*) were prepared as described by Ono and Inoue (*25*). Spinach in which nitrogen was globally replaced with ^{15}N was hydroponically cultured in medium containing $K^{15}NO_3$ and $Ca(^{15}NO_3)_2$ as nitrogen sources. To examine the H−D exchange in OEC, PS II membranes suspended in D_2O buffer (pD 5.5), including 40 mM Mes, 400 mM sucrose, 20 mM NaCl, and 20 mM $CaCl_2$, were incubated at 6 °C for 24 h. A histidine-tolerant strain of the cyanobacterium *Synechocystis* PCC 6803 was isolated as described previously (*18*). Cells of this strain were grown photoautotrophically at 30 °C for 5 days in 10 L carboys by using cool-white fluorescent lamps (7 W/m^2). BG-11 medium (*26*) was supplemented with either 0.24 mM DL-histidine containing only natural-abundance ^{14}N or 0.24 mM DL-histidine containing two ^{15}N atoms in its imidazole group. The growth medium was bubbled with 5% CO_2 in air. Under these experimental conditions, approximately 85% of the histidine molecules incorporated into thylakoid proteins were from the histidine supplemented in the growth medium as shown previously by mass analysis of histidine (*18*). Oxygen-evolving PS II core complexes from *Synechocystis* were purified as described by Tang and Diner (*27*).

FTIR spectra were measured on a JEOL JIR-6500 or a Bruker IFS-66/S spectrophotometer equipped with an MCT detector. S_2/S_1 difference spectra were measured as described previously (*21*−*23*). Spinach membranes were suspended in 40 mM Mes-NaOH (pH 5.5) buffer containing 400 mM sucrose, 20 mM NaCl, 20 mM $CaCl_2$, 18 mM potassium ferrocyanide, and 2 mM potassium ferricyanide, and sedimented by centrifugation. The pellet was then squeezed between a pair of BaF_2 plates. The sample was loaded so that the absorbance at the selected wavenumber regions of 1000−1200 and 2400−2850 cm^{-1} did not exceed 0.8. At that moment, the absorbance of the band in the amide I region around 1650 cm^{-1} was about 1.6. *Synechocystis* PS II core complexes were suspended in 5 mM Mes-NaOH (pH 6.0) buffer containing 50 mM sucrose, 5 mM NaCl, and 5 mM $CaCl_2$, and concentrated to about 6 mg of Chl/mL. An aliquot of core suspension (5 μL) was mixed with 4 μL of ferricyanide/ferrocyanide (2 mM/18 mM) solution, lightly dried on a BaF_2 plate under N_2 gas flow passed through water, and covered with another BaF_2 plate. The absorbance of the amide I band around 1650 cm^{-1} was below 1.0. The sample temperature was adjusted to 250 K in a liquid N_2 cryostat (Oxford model DN1704) equipped with ZnSe and KRS-5 windows. Two single-beam spectra (150−200 s accumulation for each) were measured before and 10 s after single-pulse illumination from a frequency-doubled Nd:YAG laser (Quanta-Ray model GCR-130; 532 nm, 7 ns pulse width, 20 mJ pulse/cm^2 at the sample point), and the difference spectrum was calculated by subtracting the spectrum obtained before from that obtained after illumination. The interval of 10 s after illumination was taken to ensure that there was no contamination by $Y_Z^{\bullet}/Y_Z$ signals and to complete electron abstraction by ferricyanide on the electron acceptor side. The spectral resolution was 4 cm^{-1}. Several spectra were averaged for the final data.

The Fe^{2+}/Fe^{3+} difference spectrum of Mn-depleted PS II core complexes from *Synechocystis* was measured following the method by Hienerwadel and Berthomieu (*28*). Manganese was depleted using 10 mM NH_2OH. An aliquot of core suspension (6 mg of Chl/mL, 5 μL) in 5 mM Mes-NaOH (pH 6.0) buffer containing 50 mM sucrose, 5 mM NaCl, and 5 mM $CaCl_2$ was mixed with 3 μL of 20 mM ferricyanide and then lightly dried on a CaF_2 plate. The absorbance of the amide I band around 1650 cm^{-1} was 0.9. The sample

temperature was maintained at about 4 °C by circulating chilled water through a copper holder. The Fe^{2+}/Fe^{3+} spectrum was taken as the difference between two single-beam spectra (10 s scans each) measured before and 2 s after flash illumination from a Nd:YAG laser (532 nm, 3 mJ/cm^2). Under this condition, signals of the electron donor side were eliminated by re-reduction of $Y_Z^{\bullet}$ by ferrocyanide, which had been produced during preoxidation of the non-heme iron by ferricyanide. The reaction was cycled with an interval of 80 s between flashes, and spectra measured over the course of 12 h were averaged. The spectral resolution was 4 cm^{-1}.

FTIR spectra of 4- and 5-MeIm and DL-histidine were measured at room temperature unless otherwise stated. Solution samples were measured between a pair of ZnSe plates with an optical path of ~7 μm. 4-MeIm (0.5 M) or DL-histidine (0.2 M) was dissolved in $H(D)_2O$ and 1 M H(D)-Cl in neutral and imidazolium forms, respectively. In aqueous solution, 4-MeIm is in tautomeric equilibrium with 5-MeIm. For an imidazolate form, 4-MeIm (0.2 M) or DL-histidine (0.2 M) was dissolved in 5 M NaOH(D) solution. The spectrum of each solvent was measured and subtracted from that of the sample to eliminate high background absorption. Crystalline DL-histidine was measured as a KBr disk. Crystalline N-deuterated DL-histidine was prepared by re-crystallization from a D_2O solution. The spectral resolution was 2 cm^{-1}.

RESULTS

Identification of a Histidine Band around 1100 cm^{-1}. Figure 2a shows flash-induced FTIR difference spectra (1200−1800 cm^{-1}) upon the S_1-to-S_2 transition of the OEC measured using PS II membranes from unlabeled and globally ^{15}N-labeled spinach (solid and dotted lines, respectively). The spectra in this region exhibit only the OEC signals, because ferricyanide in the sample functions as an exogenous electron acceptor and the non-heme iron, which could be an endogenous electron acceptor if preoxidized, was maintained in a reduced state by controlling the pH (pH 5.5) of the buffer and its redox potential using ferrocyanide (ferrocyanide:ferricyanide ratio of 9:1) (*29*). Because this study focused on relatively weak bands in the regions of 1000−1200 and 2400−2850 cm^{-1} (vide infra), the PS II sample was loaded with an amount such that the absorption at the amide I peak (~1650 cm^{-1}) was saturated ($A \approx 1.6$). Hence, the relative intensities of the bands were not reliable around 1650 cm^{-1}, although the overall features of the spectrum and the peak positions were identical to those reported (*21*, *22*). Signals were prominent in the amide I region (1600−1700 cm^{-1}), in the amide II and asymmetric carboxylate stretching region (1500−1600 cm^{-1}), and in the symmetric carboxylate stretching region (1350−1450 cm^{-1}) (*21*, *22*). Upon ^{15}N-labeling, significant changes around 1550 cm^{-1} were caused by the contribution of the amide II bands (coupled mode of N−H bending and C−N stretching vibrations) of backbone amides (*22*).

Metal complexes with histidine ligands have been reported to exhibit characteristic FTIR signals of the imidazole ring around 1100 cm^{-1} upon redox change of the metal ion (*28*−*30*). The oxidized-minus-reduced FTIR difference spectrum of the bis(4-methylimidazole) complex of iron protoporphyrin IX [FePP(4-MeIm)$_2$] exhibited a strong band at 1103 cm^{-1}

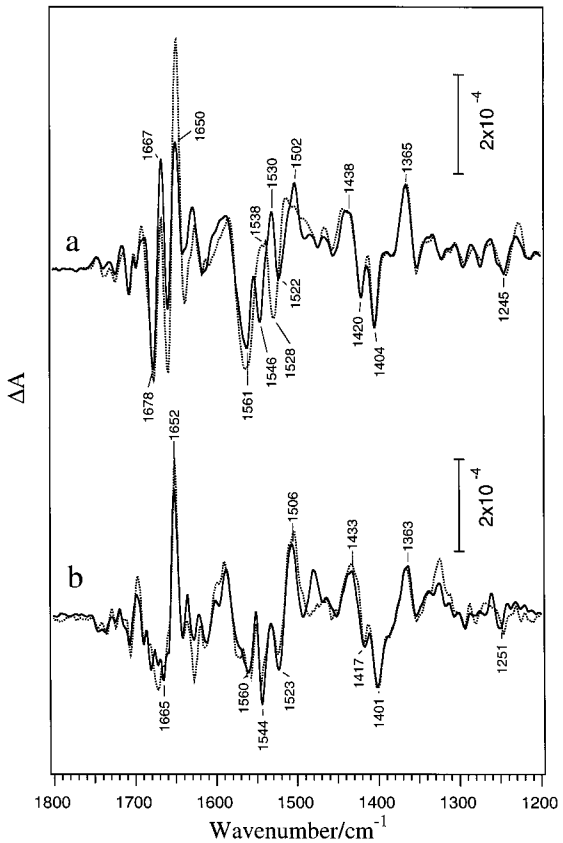

FIGURE 2: Flash-induced S_2/S_1 FTIR difference spectra (1200−1800 cm^{-1}) of the OEC in PS II preparations: (a) PS II membranes from unlabeled (solid line) and globally ^{15}N-labeled spinach (dotted line) and (b) PS II core complexes from unlabeled *Synechocystis* 6803 cells (solid line) and from cells in which both imidazole nitrogen atoms of histidine were selectively labeled with ^{15}N (dotted line). Samples included ferri- and ferrocyanide (1:9). The sample temperature was 250 K, and a difference spectrum was obtained as an after-minus-before single-pulse illumination (532 nm, 7 ns). The spectral resolution was 4 cm^{-1}.

(*30*). A similar band at 1104 cm^{-1} appeared in the same type of difference spectrum obtained from isolated Cyt b_{559} of PS II (*30*). The light-induced difference spectrum of the non-heme iron of PS II (Fe^{2+}/Fe^{3+}) (*28*, *29*) also exhibited prominent bands at 1111/1102 and 1094 cm^{-1}, which have been assigned to the neutral and deprotonated forms of histidine, respectively (*28*). Thus, a band representing a histidine side chain around 1100 cm^{-1} should also appear in the S_2/S_1 difference spectrum if the histidine ligand is attached to the redox-active Mn ion in OEC.

The spectral region of 1050−1150 cm^{-1} of the S_2/S_1 spectra of PS II membranes from unlabeled and ^{15}N-labeled spinach is presented in traces a and b of Figure 3, respectively. A dark-minus-dark difference spectrum of unlabeled PS II membranes is also presented in Figure 3c, showing the noise level of the S_2/S_1 spectra in Figure 3a. The most prominent change upon ^{15}N-labeling was the shift of a negative band at 1114 cm^{-1} to a lower frequency by 7 cm^{-1} (Figure 3a,b). This downshift value was the same as those of the 1111/1102 and 1094 cm^{-1} bands observed in the Fe^{2+}/Fe^{3+} spectrum of PS II and a band at 1066 cm^{-1} of imidazole upon ^{15}N-labeling (*28*). Thus, the band at 1114 cm^{-1} in the S_2/S_1 spectrum probably represented the imidazole mode of a histidine side chain. A positive counterpart of the negative band at 1114 cm^{-1} was not discernible around

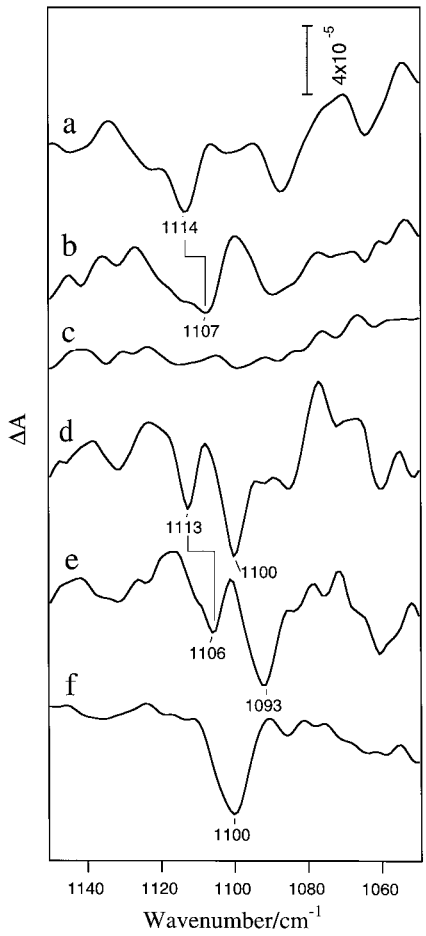

FIGURE 3: Flash-induced S_2/S_1 FTIR difference spectra (1050−1150 cm^{-1}) of PS II membranes from unlabeled (a) and globally ^{15}N-labeled spinach (b) and S_2/S_1 spectra of PS II core complexes from unlabeled *Synechocystis* cells (d) and from cells in which both the imidazole nitrogens of histidine were selectively labeled with ^{15}N (e). The measuring conditions were the same as those described in the legend of Figure 2. (c) Dark-minus-dark difference spectrum of unlabeled PS II membranes representing the noise level of spectrum a. All conditions were the same as those described for spectrum a except for the absence of illumination. (f) Flash-induced Fe^{2+}/Fe^{3+} difference spectrum of Mn-depleted PS II core complexes from unlabeled *Synechocystis* cells. The sample included ferricyanide. The spectrum was measured at 4 °C, and the resolution was 4 cm^{-1}.

1100 cm^{-1}, suggesting that the 1114 cm^{-1} band was due to an intensity change of the underlying original band rather than to a shift in peak position. This is in agreement with the reported examples of $FePP(4\text{-}MeIm)_2$, Cyt b_{559}, and Fe^{2+}/Fe^{3+} of PS II, in which the intensity of the imidazole band around 1100 cm^{-1} changed upon a redox change of the metal ion (*28*−*30*).

Since in the above experiment, nitrogen atoms in the PS II membranes were globally labeled with ^{15}N, the possibility that the shifted band arose from moieties other than imidazole that included nitrogen cannot be excluded. Hence, for definitive assignment of the band to histidine, a spectrum of the PS II sample in which only histidine side chains are isotope labeled must be measured. We measured the spectrum under such conditions using PS II core complexes from the cyanobacterium *Synechocystis* PCC 6803. Figure 2b shows S_2/S_1 spectra (1200−1800 cm^{-1}) of the PS II core complexes from unlabeled *Synechocystis* cells (solid line) and from cells in which both the imidazole nitrogens of histidine were selectively labeled with ^{15}N (dotted line). The spectral features were basically the same as those of spinach (Figure 2a), although the amide I region differed somewhat, probably due to species specificity (higher plants vs cyanobacteria) and the nature of the preparations (membranes vs core complexes). In contrast to global ^{15}N-labeling of the spinach membranes (Figure 2a), selective ^{15}N-labeling of histidine in the *Synechocystis* core complexes did not significantly change the S_2/S_1 spectrum (Figure 2b). This observation confirms the notion that most of the changes that occurred in spinach membranes upon global ^{15}N-labeling (Figure 2a) are due to isotopic substitution of the backbone nitrogen atoms. The S_2/S_1 spectra of the *Synechocystis* core complexes included some contamination by acceptor-side signals, which are typically seen at about 1480 cm^{-1} due to Q_A^-/Q_A (*31*, *32*) and at about 1330 cm^{-1} due to Fe^{2+}/Fe^{3+} (*28*, *29*) (Figure 2b). Since Q_B was absent in this core preparation, electron abstraction from Q_A by ferricyanide may be more difficult than in the membrane preparation, causing a small amount of Q_A^- to remain during the measurement. Also, modification of the Q_B-binding site may affect the redox potential of the non-heme iron, and some of the iron centers are preoxidized to become functional as an endogenous electron acceptor in PS II. The contamination by Fe^{2+}/Fe^{3+} signals was also seen in the region around 1100 cm^{-1} (vide infra). Amounts of contamination varied among spectra, resulting in small differences in intensity at about 1480 and 1330 cm^{-1} (Figure 2b). Because of interference from these contaminating signals, histidine bands could not be unambiguously identified at 1200−1800 cm^{-1} by taking the double difference between the two spectra in Figure 2b.

The S_2/S_1 spectrum in the region around 1100 cm^{-1} of unlabeled PS II core complexes from *Synechocystis* is presented in Figure 3d. A negative band at 1113 cm^{-1} corresponded to the 1114 cm^{-1} band of spinach PS II membranes (Figure 3a). This band was clearly downshifted by 7 cm^{-1} upon [^{15}N]His labeling (Figure 3e), providing definitive evidence that the band arises from the vibrational mode of the imidazole ring of histidine.

In the S_2/S_1 spectrum of *Synechocystis* (Figure 3d), there was another prominent band at 1100 cm^{-1}, which was absent in the spectrum of the PS II membranes from spinach (Figure 3a). This band was also downshifted by 7 cm^{-1} upon [^{15}N]-His labeling (Figure 3e). The same band appeared at 1100 cm^{-1} in the Fe^{2+}/Fe^{3+} spectrum measured using Mn-depleted core complexes of *Synechocystis* (Figure 3f). Therefore, the 1100 cm^{-1} band in the S_2/S_1 spectrum in Figure 3d originated from histidine ligands of the non-heme iron that arose as contamination from Fe^{2+}/Fe^{3+} signals. This frequency of 1100 cm^{-1} is slightly lower than that of the 1103 cm^{-1} band in the spinach membranes at a similar pH (pH 5.5−6.5) (*29*), suggesting structural perturbation around the iron center in the core preparation of *Synechocystis*. Such a disturbance could change the redox potential and hence produce a population of preoxidized iron centers. As judged from described S_2Fe^{2+}/S_1Fe^{3+} spectra (*29*), contamination by the non-heme iron signals accounted for less than 20% of the full population. We emphasize that the 1113 cm^{-1} band assigned to the S_2/S_1 signal of OEC was absent in the spectrum of the Mn-depleted PS II (Figure 3f). Although the observation that the contamination signal of the non-heme iron at 1100 cm^{-1} is larger than the 1113 cm^{-1} signal

of S_2/S_1 seems odd, it is explained by the fact that four histidine ligands contribute to one non-heme iron center. In addition, the signal intensity in a difference spectrum generally does not directly reflect the intensity of the original band.

Model Compounds of a Histidine Side Chain and the Effect of N-Deuteration. The imidazole side chain of histidine in its neutral state can take two tautomeric forms depending on the site of protonated nitrogen. These are Nτ-protonated (Figure 1a) and Nπ-protonated forms (Figure 1b). When both nitrogen sites are protonated and deprotonated, the histidine side chain assumes cationic imidazolium (Figure 1c) and anionic imidazolate forms (Figure 1d), respectively. A simple model compound of the histidine side chain, 4-methylimidazole (MeIm), is in tautomeric equilibrium with 5-MeIm in aqueous solution. The structures of 4- and 5-MeIm correspond to Nτ- and Nπ-protonated forms of histidine, respectively (Figure 1a,b). FTIR bands around 1100 cm^{-1} of 4- and 5-MeIm in H_2O measured at 278 K are shown in Figure 4a (thin line). Two bands of nearly equal intensity appeared at 1087 and 1104 cm^{-1}. These bands have been attributed to 4- and 5-MeIm, respectively (*33*). In fact, only the band at 1087 cm^{-1} is observed in crystalline 4-MeIm (*33*). According to the recent vibrational analysis by Majoube et al. (*33*), the 1087 cm^{-1} band of 4-MeIm and the 1104 cm^{-1} band of 5-MeIm arise mainly from C5−N1 stretching vibration. (See Figure 1a for the numbering of atoms. The numbering of 5-MeIm follows that of 4-MeIm in this study for simplicity. The C5−N1 bond in 5-MeIm corresponds to the C4−N3 bond in the original numbering of 5-MeIm in ref *33*.) An FTIR spectrum of the N-deuterated forms of 4- and 5-MeIm measured in D_2O solution at 278 K (Figure 4a, thick line) exhibited two bands at 1097 and 1103 cm^{-1}. When the temperature of the solution was lowered to 77 K, the equilibrium of the two tautomers changed and the relative intensity of the lower frequency band at 1097 cm^{-1} in D_2O as well as the band at 1087 cm^{-1} in H_2O (1090 cm^{-1} at 77 K) decreased (Figure 4b). This suggests that the bands at 1097 and 1103 cm^{-1} in D_2O correspond to the bands at 1087 and 1104 cm^{-1} in H_2O, respectively. These results indicate that the C−N band of 4-MeIm upshifts by 10 cm^{-1} upon N-deuteration while that of 5-MeIm is essentially unaffected by N-deuteration.

This assignment of N-deuterated 4- and 5-MeIm was confirmed by measurements of DL-histidine. An FTIR spectrum of DL-histidine in H_2O revealed two bands at 1090 and 1106 cm^{-1} (Figure 4e, thin line), which were assigned to Nτ- and Nπ-protonated histidine, respectively. Upon N-deuteration (Figure 4e, thick line), the major band at 1090 cm^{-1} shifted to 1096 cm^{-1}, whereas the minor band at 1106 cm^{-1} was essentially unaffected. Furthermore, crystalline DL-histidine, which has an Nτ-protonated form (*34*), exhibited only the lower-frequency band at 1093 cm^{-1}, which shifted upward by 5 cm^{-1} upon N-deuteration (Figure 4f). From these observations, it is concluded that the C−N band at 1087−1093 cm^{-1} of Nτ-protonated histidine or 4-MeIm upshifts by 5−10 cm^{-1} upon N-deuteration, whereas the band at 1103−1106 cm^{-1} of Nπ-protonated histidine or 5-MeIm is essentially insensitive to N-deuteration.

Traces c and g of Figure 4 (thin line) are FTIR spectra of 4-MeIm and DL-histidine, respectively, in 1 M HCl. Under acidic conditions, both imidazole nitrogen atoms are protonated and an imidazolium form is produced (Figure 1c). As expected, only one band appeared at 1089 cm^{-1} in 4-MeImH$^+$ and at 1094 cm^{-1} in HisH$^+$. These bands were located at frequencies slightly higher than those of the Nτ-protonated forms of respective compounds measured at similar temperatures (traces a and e of Figure 4). Upon N-deuteration, the bands shifted upward by 19 and 16 cm^{-1} in 4-MeImD$^+$ and DL-HisD$^+$, respectively (traces c and g of Figure 4, thick line). These shifts were about twice as large as those of the Nτ-protonated neutral form (5−10 cm^{-1}).

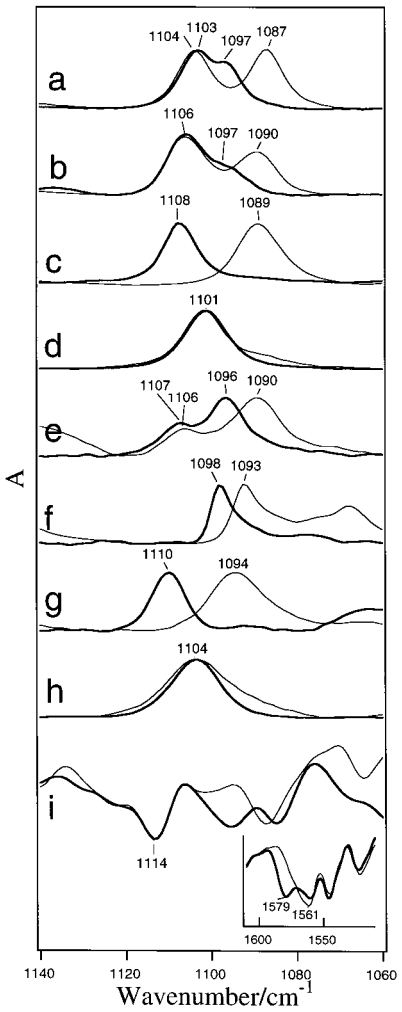

FIGURE 4: C−N stretching region (1060−1140 cm^{-1}) of FTIR spectra of 4- and 5-MeIm (a−d) and DL-histidine (e−h) and the S_2/S_1 difference spectra of OEC (i). Each panel shows one spectrum in H_2O (or N-protonated form) (thin line) and another in D_2O (or N-deuterated form) (thick line). (a and b) 4- and 5-MeIm (0.5 M) in $H(D)_2O$ at 278 (a) and 77 K (b). 4-MeIm is in tautomeric equilibrium with 5-MeIm in $H(D)_2O$. (c) 4-MeImH(D)$^+$ (0.5 M) in 1 M H(D)Cl. (d) 4-MeIm$^-$ (0.2 M) in 5 M NaOH(D). (e) DL-His (0.2 M) in $H(D)_2O$. (f) Crystalline DL-His and its N-deuterated form. (g) DL-HisH(D)$^+$ (0.2 M) in 1 M H(D)Cl. (h) DL-His$^-$ (0.2 M) in 5 M NaOH. Spectra c−h were measured at room temperature. (i) S_2/S_1 spectra of PS II membranes from spinach in $H(D)_2O$ buffer measured at 250 K. The inset shows the asymmetric carboxylate stretching region of the S_2/S_1 spectra, showing the 1579 cm^{-1} band characteristic of the deuterated OEC (*22*).

4-MeIm (Figure 4d, thin line) and DL-histidine (Figure 4h, thin line) in 5 M NaOH exhibit bands at 1101 and 1104 cm^{-1}, respectively. Under alkaline conditions, the imidazole ring is deprotonated and an imidazolate form is produced (Figure 1d). These frequencies were slightly lower than those

of the Nπ-protonated forms of each compound (traces a and e of Figure 4). The frequency did not shift when these compounds were dissolved in NaOD (traces d and h of Figure 4, thick line), in agreement with the absence of protons in the imidazolate form.

The effect of H−D exchange on the histidine band at 1114 cm^{-1} in the S_2/S_1 difference spectrum of the PS II membranes is shown in Figure 4i. Sufficient deuteration of OEC was confirmed by the appearance of the 1579 cm^{-1} band (inset), which is typical of a deuterated S_2/S_1 spectrum and has been attributed to the asymmetric stretch of a carboxylate ligand strongly hydrogen-bonded with water (*22*). The 1114 cm^{-1} band in H_2O buffer (Figure 4i, thin line) was not affected by deuteration (Figure 4i, thick line). The 1113 cm^{-1} band of *Synechocystis* core complexes (Figure 3d) also did not change upon H−D exchange (data not shown). This insensitivity to deuteration agrees with the results of the Nπ-protonated and imidazolate forms of histidine. Note that the other changes in this region caused by H−D exchange (e.g., the band appearing at 1095 cm^{-1}; Figure 4i) probably arose from other protein bands that are sensitive to deuteration. Only the 1114 cm^{-1} band was definitely assigned to histidine in this spectral region (vide supra).

Hydrogen-Bonding N−H Stretching Region. When an N−H group of imidazole compounds is involved in strong hydrogen bonding, a broad N−H stretching band appears around 2800 cm^{-1} with a number of sub-bands, while an N−H group free from hydrogen bonding exhibits a narrow band at about 3500 cm^{-1} (*33*, *35*−*38*). These sub-bands have been explained to arise from Fermi resonance of overtones or combinations of fundamental vibrations with the superimposing N−H stretching vibration (*35*−*37*). Figure 5 shows S_2/S_1 difference spectra in the region between 2400 and 2850 cm^{-1}. The spectrum of unlabeled PS II membranes from spinach (Figure 5a) shows a structure with positive or negative peaks at 2806, 2765, 2758, 2727, 2692, 2638, 2613, and 2584 cm^{-1} on a broad positive background. Figure 5c shows the noise level of this spectrum as a dark-minus-dark difference spectrum. Frequency regions above 2850 cm^{-1} cause extremely high noise due to water absorption and thus are not shown in Figure 5. Upon global ^{15}N-labeling of the PS II membranes, all the above peaks downshifted by 10−30 cm^{-1} (Figure 5b). The S_2/S_1 spectrum of PS II core complexes from *Synechocystis* (Figure 5d) contained peaks at positions similar to those of the spinach membranes with a similar broad background. These peaks also downshifted upon [^{15}N]His labeling (Figure 5e), like they did upon global ^{15}N-labeling. Although the S_2/S_1 spectra of the *Synechocystis* core complexes include some contamination from non-heme iron signals as described above, the Fe^{2+}/Fe^{3+} spectrum measured with Mn-depleted core complexes (Figure 5f) did not reveal either detectable peaks or a broad background. It is noted that because the non-heme iron center seemed rather modified in this core complex of *Synechocystis*, further studies are necessary to confirm the absence of bands in this region of an intact Fe^{2+}/Fe^{3+} spectrum.

The above results indicate that the peaks observed in the region of 2500−2850 cm^{-1} originated from the histidine side chain in OEC and can be ascribed to Fermi resonance peaks on a hydrogen-bonding N−H stretching band. The presence of these peaks provides evidence that at least one of the two imidazole nitrogens is protonated (i.e., not in the imidazolate form) and that this N−H group is hydrogen bonded.

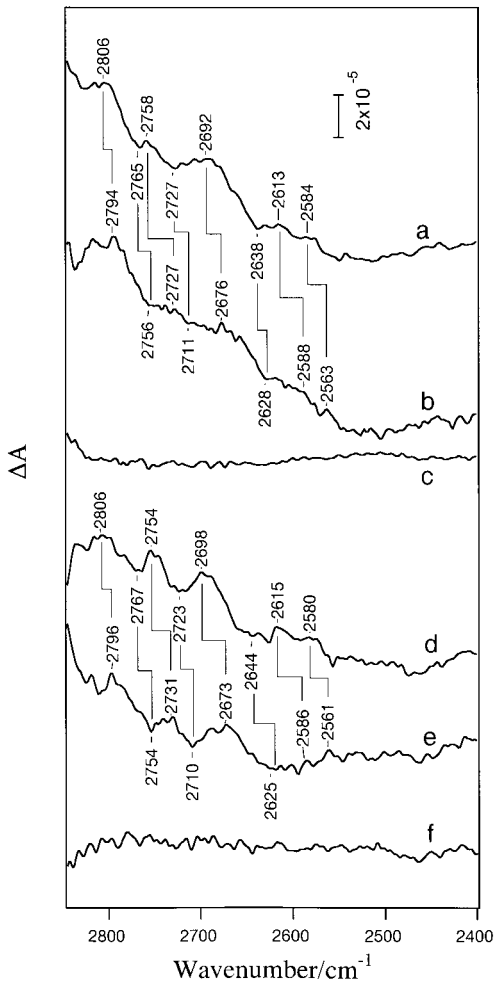

FIGURE 5: Flash-induced S_2/S_1 FTIR difference spectra (2400−2850 cm^{-1}) of PS II membranes from unlabeled (a) and globally ^{15}N-labeled spinach (b). S_2/S_1 spectra of PS II core complexes from unlabeled *Synechocystis* cells (d) and from cells in which both imidazole nitrogen atoms of histidine were selectively labeled with ^{15}N (e). Measuring conditions were the same as those described in the legend of Figure 2. (c) Dark-minus-dark difference spectrum of unlabeled PS II membranes representing the noise level of spectrum a. All conditions were the same as those described for spectrum a except for the absence of illumination. (f) Flash-induced Fe^{2+}/Fe^{3+} difference spectrum of Mn-depleted PS II core complexes form unlabeled *Synechocystis* cells. Measuring conditions were the same as those described in the legend of Figure 3f. The spectrum was normalized with spectrum d to adjust the intensity of the histidine peak at 1100 cm^{-1} (Figure 3d,f).

Several explanations can account for the origin of the broad background observed in frequencies above 2500 cm^{-1} (traces a, b, d, and e of Figure 5). One is the N−H stretching band itself that should underlie the Fermi resonance peaks. Stronger hydrogen bonding of the histidine N−H upon S_2 formation will shift the broad N−H band to a lower frequency with an increase in intensity, which could result in the broad positive feature seen in Figure 5. Another possibility is that this band arises from N−H groups other than histidine or the O−H groups of water and proteins. The broad feature could result from local changes in hydrogen bonding interactions among these groups or from overall changes in the hydrogen bonding network as seen in various strongly hydrogen-bonding systems (*39*). Indeed, Breton and Nabedryk (*40*) recently observed broad positive bands in the

Table 1: Frequencies of C−N Stretching Bands of 4- and 5-Methylimidazole and Histidine

	H_2O solution or N−H form	D_2O solution or N−D form	shift upon N-deuteration	protonated nitrogen(s)
4,5-MeIm in $H(D)_2O$ at 278 K	1087	1097	10	Nτ (4-MeIm)
	1104	1103	−1	Nπ (5-MeIm)
4,5-MeIm in $H(D)_2O$ at 77 K	1090	1097	7	Nτ (4-MeIm)
	1106	1106	0	Nπ (5-MeIm)
$MeImH(D)^+$ in H(D)Cl solution	1089	1108	19	Nτ, Nπ
$MeIm^-$ in NaOH(D) solution.	1101	1101	0	no protonation
DL-His in $H(D)_2O$	1090	1096	6	Nτ
	1106	1107	1	Nπ
crystalline DL-His	1093	1098	5	Nτ
DL-$HisH(D)^+$ in H(D)Cl solution	1094	1110	16	Nτ, Nπ
DL-His^- in NaOH(D) solution	1104	1104	0	no protonation
FePP(4-MeIm)$_2$ at pH(D) 8[a]	1103	1103	0	Nπ
FePP(4-MeIm)$_2$ at pH 12[a]	1099	−	−	no protonation
Cyt b_{559} (isolated) of PS II at pH(D) 6.4[a]	1104	1104	0	Nπ
Fe^{2+}/Fe^{3+} of PS II at pH 5.5[b]	1111/1103	−	−	Nπ
Fe^{2+}/Fe^{3+} of PS II at pH(D) 8[c]	1111/1102	1110/1103	−1/1	Nπ
	1094	1093	−1	no protonation
OEC (S_2/S_1) of spinach at pH 5.5	1114	1114	0	Nπ
OEC (S_2/S_1) of *Synechocystis* at pH 6.0	1113	1113	0	Nπ

[a] Berthomieu et al. (*30*). [b] Noguchi and Inoue (*29*). [c] Hienerwadel and Berthomieu (*28*).

region of 2400−3000 cm^{-1} in Q_A^-/Q_A and Q_B^-/Q_B difference spectra of bacterial reaction centers and interpreted them as being due to the redistribution of protons in a large web of polarizable hydrogen bonds.

DISCUSSION

IR Markers of Protonation Forms and Hydrogen Bonding of a Histidine Side Chain. (1) C−N Stretching Band around 1100 cm^{-1}. Previous Raman studies have shown that the C4═C5 stretching band of the histidyl imidazole ring in the region of 1565−1610 cm^{-1} can be used as a marker with which to distinguish Nτ- and Nπ-protonated forms (*41*, *42*). However, the IR spectra of proteins generally have a high level of absorption at this frequency due mainly to amide II and carboxylate stretching bands. Therefore, the C4═C5 band is not a useful marker of histidine structure in proteins when using FTIR spectroscopy. This study shows that the C−N stretching band around 1100 cm^{-1} can be a useful IR determinant of the protonation form of a histidine side chain (Figure 4 and Table 1). FTIR measurements for the model compounds, 4- and 5-MeIm and DL-histidine, indicated that the Nπ-protonated form (Figure 1b) has a band at 1104−1106 cm^{-1}, while the Nτ-protonated form (Figure 1a) has a band at the lower frequency of 1087−1093 cm^{-1}. Also, the imidazolium form (Figure 1c) has a band at a frequency slightly higher than that of the Nτ-protonated form, while the imidazolate form (Figure 1d) has a band at a slightly lower frequency than the Nπ-protonated form. Thus, the order of C−N frequencies of the imidazole ring of histidine tends to be as follows: Nπ-protonated (>1100 cm^{-1}) > imidazolate > imidazolium > Nτ-protonated (<1095 cm^{-1}).

Other studies of imidazole−metal complexes in model compounds and proteins also show this tendency (Table 1). FePP(4-MeIm)$_2$ at pH 8 (*30*), isolated Cyt b_{559} of PS II at pH 6.4 (*30*), and the non-heme iron of PS II at pH 5.5 (*29*), in which imidazole ligands are considered to take an Nπ-protonated form, have C−N stretching bands at 1103−1111 cm^{-1} in FTIR difference spectra upon a redox change of the central metal. When the pH is increased, the C−N frequency of FePP(4-MeIm)$_2$ (pH 12) decreases to 1099 cm^{-1} (*30*) and the non-heme iron of PS II (pH 8) exhibits an additional signal at 1094 cm^{-1} (*28*). These decreases in frequency are thought to result from imidazolate formation (*28*, *30*). Thus, metal binding does not seem to induce a significant change in C−N frequency. In other words, the C−N frequency is primarily determined by the protonation structure. Metal coordination may affect the C−N vibration in a finer way, but further detailed studies are necessary to elucidate this coordination effect.

The effect of N-deuteration on the C−N band more clearly distinguishes the protonation forms of histidine (Figure 4 and Table 1). While the frequency of the Nπ-protonated form was little affected by N-deuteration (less than ±1 cm^{-1}), the Nτ-protonated form exhibited an upshift of 5−10 cm^{-1} upon N-deuteration. The upshift of the imidazolium form was even larger (16−19 cm^{-1}), whereas N-deuteration did not affect the frequency of the imidazolate form because attached protons were absent. These results indicate that the tendency of the N-deuteration effect on the C−N stretching frequency of histidine can be summarized as follows: imidazolium (15−20 cm^{-1}) > Nτ-protonated (5−10 cm^{-1}) > Nπ-protonated ≈ imidazolate (∼0 cm^{-1}). This relationship holds even when the imidazole ring coordinates a metal ion, as seen in FePP(4-MeIm)$_2$, isolated Cyt b_{559} of PS II (*30*), and the non-heme iron of PS II (*28*) (Table 1).

The above N-deuteration effect can be explained by normal mode assignment. The bands around 1100 cm^{-1} of 4- and 5-MeIm are mainly caused by the C5−N1 stretching vibration (*33*) (see Figure 1a for numbering). This vibration will be affected by deuteration at the N1 site in the Nτ(N1)-protonated form (Figure 1a), but will be rather insensitive to deuteration at N3 in the Nπ(N3)-protonated form (Figure 1b). The upshifting tendency of the C5−N1 band upon N1-deuteration may result from decoupling of the mixed N−H bending vibration upon deuteration. Indeed, normal mode calculation of 4-MeIm (*33*) and 4-EtIm (*43*) at the ab initio level predicted an upshift of the C5−N1 mode by 4−6 cm^{-1} upon N1-deuteration. The N-deuteration effect was almost doubled in the imidazolium, as compared with that in the Nτ-protonated form. Presumably, the C−N band around 1100

cm^{-1} of the imidazolium form includes contributions from both the C5−N1 and C4−N3 vibrations, and hence, both N1- and N3-deuteration affect frequency.

(2) Fermi Resonance Peaks on a Hydrogen-Bonding N−H Stretching Band. A hydrogen-bonding N−H stretching band exhibits a broad feature with a number of subpeaks at 2400−3300 cm^{-1}. This feature has been attributed to the Fermi resonance of overtones and combinations of imidazole ring modes with the N−H stretching vibration (*35*−*37*). While it is not easy to identify a broad hydrogen-bonding N−H band itself in proteins in aqueous solution, the presence of Fermi resonance peaks is a good indication of an underlying N−H band. Thus, Fermi resonance peaks are a useful marker of the hydrogen-bonding N−H group of a histidine side chain. Indeed, we have recently used the Fermi resonance peaks to detect a hydrogen bonding interaction between the Q_A carbonyl and the histidine N−H in PS II core complexes (*44*). Detection of an N−H group using Fermi resonance peaks can also distinguish an imidazolate form that does not have an N−H bond. This procedure is especially useful in distinguishing between the Nπ-protonated and imidazolate forms, both of which have relatively close C−N frequencies and exhibit no N-deuteration effect.

Structure of the Histidine Side Chain in the OEC. Selective ^{15}N-labeling of histidine side chains of PS II core complexes of *Synechocystis* together with global ^{15}N-labeling of PS II membranes of spinach has identified histidine signals in S_2/S_1 FTIR difference spectra. A negative band at 1113−1114 cm^{-1} (1113 cm^{-1} in *Synechocystis* and 1114 cm^{-1} in spinach), which was downshifted by 7 cm^{-1} upon ^{15}N-labeling (Figure 3), was assigned to the C−N stretching mode of a histidine side chain. Also, several peaks at 2500−2850 cm^{-1}, all of which were downshifted upon ^{15}N-labeling (Figure 5), were attributed to Fermi resonance peaks superimposed on a hydrogen-bonding N−H stretching band of the imidazole ring. The structure of the histidine side chain responsible for these signals can be determined using the above criteria. The relatively high frequency at 1113−1114 cm^{-1} and its insensitivity to H−D exchange (Figure 4i) indicated that the imidazole ring of this histidine has an Nπ-protonated form (Table 1). The observation of Fermi resonance peaks on the hydrogen-bonding N−H stretching region also confirms the presence of N−H group and provides evidence that the N−H is hydrogen bonded. This structure is considered to remain in both S_1 and S_2 states, because the negative band at 1113−1114 cm^{-1} in the S_2/S_1 difference spectrum appeared as an intensity decrease of the original band and no other signals could be assigned to histidine around 1100 cm^{-1}.

Since the S_1-to-S_2 transition is thought to be a process of one-electron oxidation of the Mn cluster (*1*−*6*), the histidine side chain affected by the S_2 formation and detected in the S_2/S_1 difference spectrum is probably a ligand of the redox-active Mn ion. The proposed structure of the histidine ligand of the Mn cluster is shown in Figure 6. The Mn ion must be attached to the Nτ site because the Nπ site is already protonated. With this structure, it is seen that the C5−N1 vibration, which is mainly responsible for the 1113−1114 cm^{-1} band, is sensitive to the redox change of the Mn ion at the N1 (Nτ) site. This histidine ligand is most likely identical to that detected by the ESEEM studies (*18*). The Nπ−H group forms a hydrogen bond with another amino acid

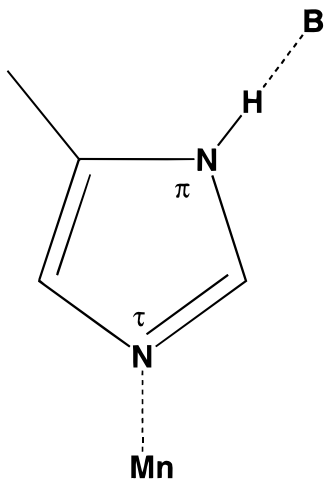

FIGURE 6: Proposed structure of a histidine ligand of the Mn cluster. B represents an unidentified hydrogen-bond acceptor.

residue or a water molecule (expressed as B in Figure 6). The possibility cannot yet be ruled out that the histidine in the S_2/S_1 spectrum is a ligand of a Ca^{2+} ion or is structurally coupled to the Mn cluster through a hydrogen bonding network. Indeed, we recently showed that signals of a tyrosine residue (most likely Y_Z), which is structurally coupled to the Mn cluster but is not a ligand, are included in the S_2/S_1 FTIR spectrum (*23*).

Site-directed mutant (*9*−*11*) and chemical modification (*13*, *15*) studies have proposed that D1-His332 and D1-His337 are candidate histidine ligands of the Mn cluster. D1-His190 has also been proposed to be a possible ligand of the Mn or an immediate proton acceptor for Y_Z (*8*, *45*, *46*). Thus, one of these residues is most likely responsible for the histidine signal observed in this study. The presence of only one histidine band of OEC near 1100 cm^{-1} does not necessarily indicate that the Mn cluster has a single histidine ligand. Because the S_2/S_1 spectrum detects only the vibrational modes affected by S_2 formation, histidine ligands of the redox-inactive Mn ions, if any, may not appear. Also, more than one histidine residue with a similar structure may contribute to the 1113−1114 cm^{-1} band.

In conclusion, FTIR signals of a histidine side chain were identified in the S_2/S_1 FTIR spectrum and its protonation structure and the nature of its hydrogen bonding interaction were determined. The IR markers of histidine presented in this study will be useful for investigating the reactions of histidine residues that are expected to be directly involved in O_2-evolving reactions in higher S states.

ACKNOWLEDGMENT

We thank Dr. R. D. Britt for providing [^{15}N]histidine.

REFERENCES

1. Debus, R. J. (1992) *Biochim. Biophys. Acta 1102*, 269−352.
2. Britt, R. D. (1996) in *Oxygenic Photosynthesis: The Light Reactions* (Ort, D. R., and Yocum, C. F., Eds.) pp 137−164, Kluwer, Dordrecht, The Netherlands.
3. Renger, G. (1997) *Physiol. Plant. 100*, 824−841.
4. Tommos, C., and Babcock, G. T. (1998) *Acc. Chem. Res. 31*, 18−25.
5. Yachandra, V. K., DeRose, V. J., Latimer, M. J., Mukerji, I., Sauer, K., and Klein, M. P. (1993) *Science 260*, 675−679.

6. Yachandra, V. K., Sauer, K., and Klein, M. P. (1996) *Chem. Rev. 96*, 2927−2950.
7. Nixon, P. J., and Diner, B. A. (1992) *Biochemistry 31*, 942−948.
8. Chu, H.-A., Nguyen, A. P., and Debus, R. J. (1995) *Biochemistry 34*, 5839−5858.
9. Chu, H.-A., Nguyen, A. P., and Debus, R. J. (1995) *Biochemistry 34*, 5859−5882.
10. Nixon, P. J., Chrisholm, D. A., and Diner, B. A. (1992) in *Plant Protein Engineering* (Shewry, P., and Gutteridge, S., Eds.) pp 93−141, Cambridge University Press, Cambridge, U.K.
11. Bowlby, N. R., Sithole, I., Babcock, G. T., and McIntosh, L. (1996) *Ber. Bunsen-Ges. Phys. Chem. 100*, 1978−1986.
12. Tamura, N., Ikeuchi, M., and Inoue, Y. (1989) *Biochim. Biophys. Acta 973*, 281−289.
13. Preston, C., and Seibert, M. (1991) *Biochemistry 30*, 9625−9633.
14. Ghirardi, M. L., Lutton, T. W., and Seibert, M. (1998) *Biochemistry 37*, 13559−13566.
15. Ghirardi, M. L., Preston, C., and Seibert, M. (1998) *Biochemistry 37*, 13567−13574.
16. DeRose, V. J., Yachandra, V. K., McDermott, A. E., Britt, R. D., Sauer, K., and Klein, M. P. (1991) *Biochemistry 30*, 1335−1341.
17. Tang, X.-S., Sivaraja, M., and Dismukes, G. C. (1993) *J. Am. Chem. Soc. 115*, 2382−2389.
18. Tang, X.-S., Diner, B. A., Larsen, B. S., Gilchrist, M. L., Lorigan, G. A., and Britt, R. D. (1994) *Proc. Natl. Acad. Sci. U.S.A. 91*, 704−708.
19. Noguchi, T., Ono, T., and Inoue, Y. (1992) *Biochemistry 31*, 5953−5956.
20. Noguchi, T., Ono, T., and Inoue, Y. (1993) *Biochim. Biophys. Acta 1143*, 333−336.
21. Noguchi, T., Ono, T., and Inoue, Y. (1995) *Biochim. Biophys. Acta 1228*, 189−200.
22. Noguchi, T., Ono, T., and Inoue, Y. (1995) *Biochim. Biophys. Acta 1232*, 59−66.
23. Noguchi, T., Inoue, Y., and Tang, X.-S. (1997) *Biochemistry 36*, 14705−14711.
24. Berthold, D. A., Babcock, G. T., and Yocum, C. F. (1981) *FEBS Lett. 134*, 231−234.
25. Ono, T., and Inoue, Y. (1986) *Biochim. Biophys. Acta 850*, 380−389.
26. Rippke, R., DeRuelles, J., Waterbury, J. B., Herdman, M., and Starkier, R. Y. (1979) *J. Gen. Microbiol. 111*, 1−61.
27. Tang, X.-S., and Diner, B. A. (1994) *Biochemistry 33*, 4595−4603.
28. Hienerwadel, R., and Berthomieu, C. (1995) *Biochemistry 34*, 16288−16297.
29. Noguchi, T., and Inoue, Y. (1995) *J. Biochem. 118*, 9−12.
30. Berthomieu, C., Boussac, A., Mäntele, W., Breton, J., and Nabedryk, E. (1992) *Biochemistry 31*, 11460−11471.
31. Berthomieu, C., Nabedryk, E., Mäntele, W., and Breton, J. (1990) *FEBS Lett. 269*, 363−367.
32. Hienerwadel, R., Boussac, A., Breton, J., and Berthomieu, C. (1996) *Biochemistry 35*, 15447−15460.
33. Majoube, M., Millié, Ph., and Vergoten, G. (1995) *J. Mol. Struct. 344*, 21−36.
34. Edington, P., and Harding, M. M. (1974) *Acta Crystallogr. B30*, 204−206.
35. Wolff, H., and Wolff, E. (1971) *Spectrochim. Acta 27A*, 2109−2118.
36. Perchard, C., and Novak, A. (1968) *J. Chem. Phys. 48*, 3079−3084.
37. Bellocq, A. M., Perchard, C., Novak, A., and Josien, M. L. (1965) *J. Chim. Phys. 62*, 1334−1343.
38. Zimmermann, H. (1961) *Z. Elektrochem. 65*, 821−840.
39. Zundel, G. (1988) *J. Mol. Struct. 177*, 43−68.
40. Breton, J., and Nabedryk, E. (1998) *Photosynth. Res. 55*, 301−307.
41. Ashikawa, I., and Itoh, K. (1979) *Biopolymers 18*, 1859−1876.
42. Miura, T., Satoh, T., Hori-i, A., and Takeuchi, H. (1998) *J. Raman Spectrosc. 29*, 41−47.
43. Gallouj, H., Lagant, P., and Vergoten, G. (1997) *J. Raman Spectrosc. 28*, 909−916.
44. Noguchi, T., Inoue, Y., and Tang, X.-S. (1999) *Biochemistry 38*, 399−403.
45. Hays, A.-M. A., Vassiliev, I. R., Golbeck, J. H., and Debus, R. J. (1998) *Biochemistry 37*, 11352−11365.
46. Mamedov, F., Sayre, R. T., and Styring, S. (1998) *Biochemistry 37*, 14245−14256.

BI990631+